

## Dynnikov coordinates on punctured torus

Alev MERAL\* 

Department of Mathematics, Faculty of Science, Dicle University, Diyarbakır, Turkey

Received: 06.10.2020

Accepted/Published Online: 14.02.2021

Final Version: 26.03.2021

**Abstract:** We generalize the Dynnikov coordinate system previously defined on the standard punctured disk to an orientable surface of genus-1 with  $n$  punctures and one boundary component.

**Key words:** Integral lamination, geometric intersection number, Dynnikov coordinates, punctured torus

### 1. Introduction

The aim of this paper is to generalize Dynnikov coordinates to a genus-1 surface with  $n$  ( $n \geq 2$ ) punctures and one boundary component. The Dynnikov coordinate system [4] is an effective way to coordinate an integral lamination on a finitely punctured disk  $D_n$  ( $n \geq 3$ ). It provides a bijection between the isotopy classes of integral laminations and  $\mathbb{Z}^{2n-4} \setminus \{0\}$ . The Dynnikov coordinate system has been extensively used to solve various dynamical and combinatorial problems such as the word problem in the braid group [2, 3], calculating the topological entropies of pseudo-Anosov braids [7, 9] and computing the geometric intersection number of two integral laminations on  $D_n$  [11].

Throughout the paper,  $S_n$  shall denote a genus-1 surface with  $n$  ( $n \geq 2$ ) punctures and one boundary component. To coordinate an integral lamination given on  $S_n$ , a system consisting of  $3n + 2$  arcs and a simple closed curve on  $S_n$  is used. Given an integral lamination  $\mathcal{L}$  (or a measured foliation  $\mathcal{F}$ ), first, we have introduced a vector in  $\mathbb{Z}_{\geq 0}^{3n+3} \setminus \{0\}$  (or  $\mathbb{R}_{\geq 0}^{3n+3} \setminus \{0\}$ ) using the geometric intersection numbers (or the measure assigned to these curves) with the curves in our system. To uniquely determine every lamination, we have defined the Dynnikov coordinates on  $S_n$  by considering the linear combinations of these intersection numbers (see Section 2).

### 2. Dynnikov coordinates on $S_n$

In this section, we describe the Dynnikov coordinates on  $S_n$ . For this, we use the model shown in Figure 1. Here the arcs  $\alpha_i$  ( $1 \leq i \leq 2n$ ) and  $\beta_i$  ( $1 \leq i \leq n + 1$ ) are similar to the  $D_n$  case. Thus, the endpoints of these arcs are either on the boundary or on the puncture. While  $c$  is the longitude of the torus,  $\gamma$  is the arc whose both endpoints are on the boundary. Moreover, note that  $\gamma$  intersects  $c$  once transversally.

Let  $\mathcal{L}_n$  be the set of integral laminations (an integral is a finite union of mutually disjoint essential simple closed curves up to isotopy; for example, you can see Figure 2) on  $S_n$  and  $\mathcal{L} \in \mathcal{L}_n$ . An integral lamination is

\*Correspondence: alev.meral@dicle.edu.tr

2010 AMS Mathematics Subject Classification: 57N05, 57N16, 57M50

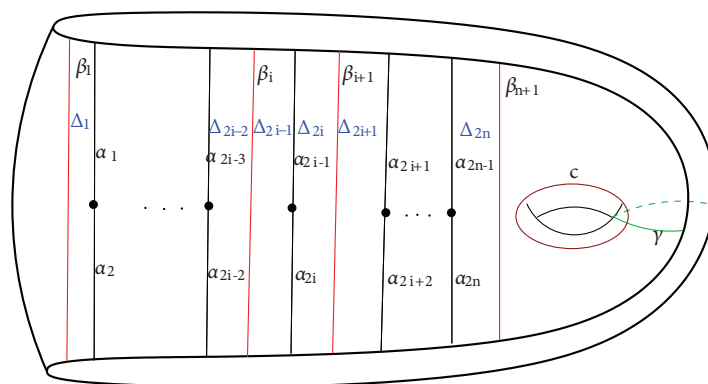


Figure 1. Curves on  $S_n$ .

generally disconnected. However, when this integral lamination consists of only one closed curve, it becomes connected. Throughout the paper, we always work with the minimal representative (an integral lamination in the same isotopy class intersecting minimally with coordinate curves) of  $\mathcal{L}$  and denote it by  $L$ . Let the vector  $(\alpha_1, \dots, \alpha_{2n}; \beta_1, \dots, \beta_{n+1}; \gamma; c) \in \{\mathbb{Z}_{\geq 0}^{3n+3}\} \setminus \{0\}$  show the intersection numbers of  $L$  with the corresponding arcs and the simple closed curve  $c$ . For example,  $(4, 1, 3, 2, 4, 1; 3, 5, 5, 3; 3; 1)$  are the intersection numbers of the integral lamination  $L$  depicted in Figure 2.

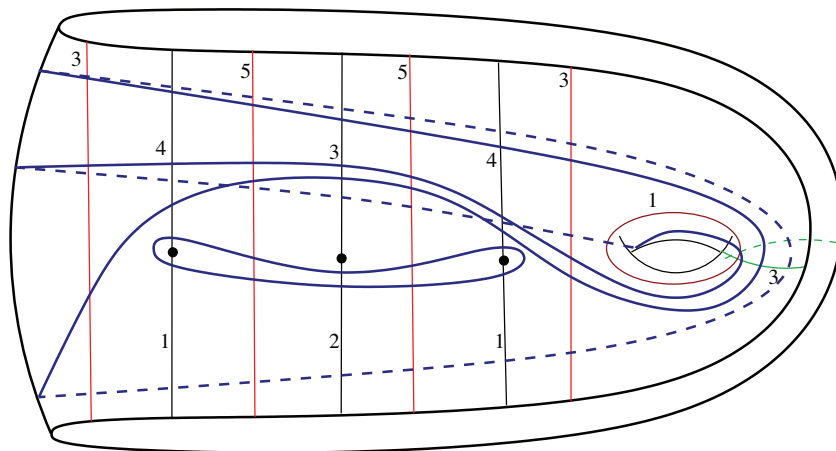


Figure 2. Intersection numbers of the integral lamination  $L$  with the coordinate curves.

### 2.1. Path components on $S_n$

In this section, we shall introduce the path components of an integral lamination  $L$  on  $S_n$  and derive formulas for the number of these components.

Let  $U_i$  ( $1 \leq i \leq n$ ) be the region that is bounded by  $\beta_i$  and  $\beta_{i+1}$  (see Figure 3) and  $G$  be the region bounded by  $\beta_1$ ,  $\beta_{n+1}$  and the boundary of  $S_n$  ( $\partial S_n$ ) (see Figures 4 and 5). Each component of  $L \cap U_i$  and  $L \cap G$  is called the path component of  $L$  in  $U_i$  and  $G$ , respectively. Since  $L$  is minimal, there are 4 types of path components in  $U_i$  ( $1 \leq i \leq n$ ) as on the disk [10] (see Figure 3). An above component has endpoints on  $\beta_i$  and  $\beta_{i+1}$  and intersects  $\alpha_{2i-1}$ . A below component has endpoints on  $\beta_i$  and  $\beta_{i+1}$  and intersects  $\alpha_{2i}$ . A left loop

component has both endpoints on  $\beta_{i+1}$  and intersects  $\alpha_{2i-1}$  and  $\alpha_{2i}$  (see Figure 3a). A right loop component has both endpoints on  $\beta_i$  and intersects  $\alpha_{2i-1}$  and  $\alpha_{2i}$  (see Figure 3b). There are 6 types of path components in  $G$ . The first three of these are curve  $c$ , front genus component and back genus component. The curve  $c$  is the longitude of the torus (see Figure 4a). The front genus component has both endpoints on  $\beta_{n+1}$  and does not intersect the curve  $c$  (see Figure 4b). The back genus component has both endpoints on  $\beta_1$  and does not intersect the curve  $c$  (see Figure 4c). The other three components are called twisting, which have endpoints on  $\beta_1$  and  $\beta_{n+1}$  and intersect the curve  $c$  (see Figure 5). These components are nontwist, negative twist, and positive twist components. The nontwist component does not make any twist (see Figure 5a). The negative twist component makes clockwise twist (see Figure 5b). The positive twist component makes counterclockwise twist (see Figure 5c).

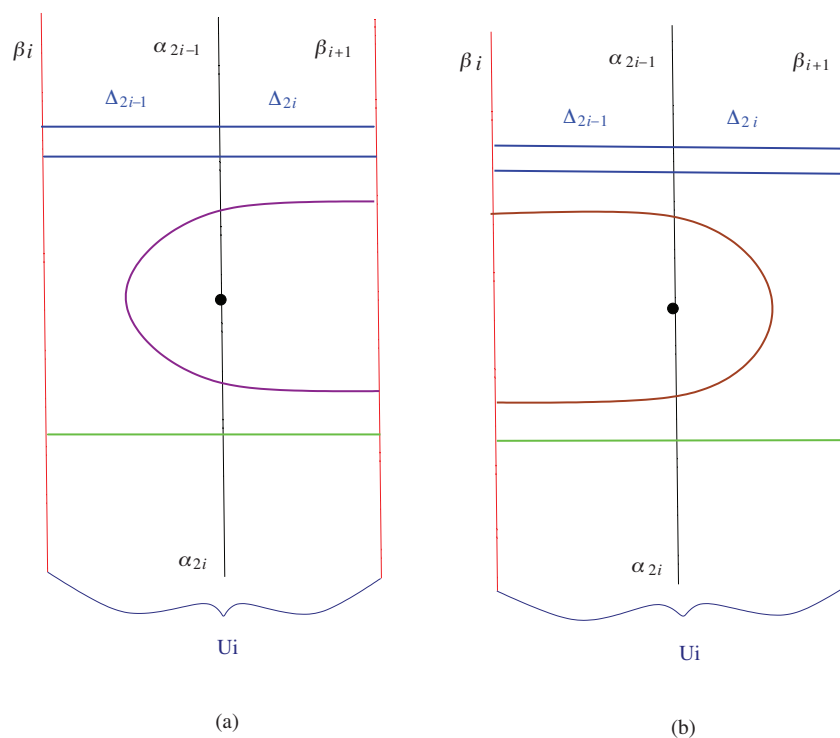


**Figure 3.** Above and below components, left and right loop components in the region  $U_i$ .

The twist number of a twisting component is the signed number of intersections with the curve  $\gamma$ .

**Remark 2.1** *Since an integral lamination  $L \in \mathcal{L}_n$  consists of simple closed curves that do not intersect each other, there cannot be both curve  $c$  and twisting components at the same time in the region  $G$  (see Figure 6). Also note that there are a monotype front genus and a monotype back genus component in the region  $G$ .*

**Remark 2.2** *If  $L$  contains the  $p(c)$  copies of the curve  $c$ , then let*

$$c = -p(c), \tag{2.1}$$

*where  $p(c) > 0$ . Moreover, let  $c^+$  give the number of the twisting components in the region  $G$ . From Remark 2.1, there cannot be both the curve  $c$  and the twisting components at the same time. Therefore,  $c^+$  is defined by*

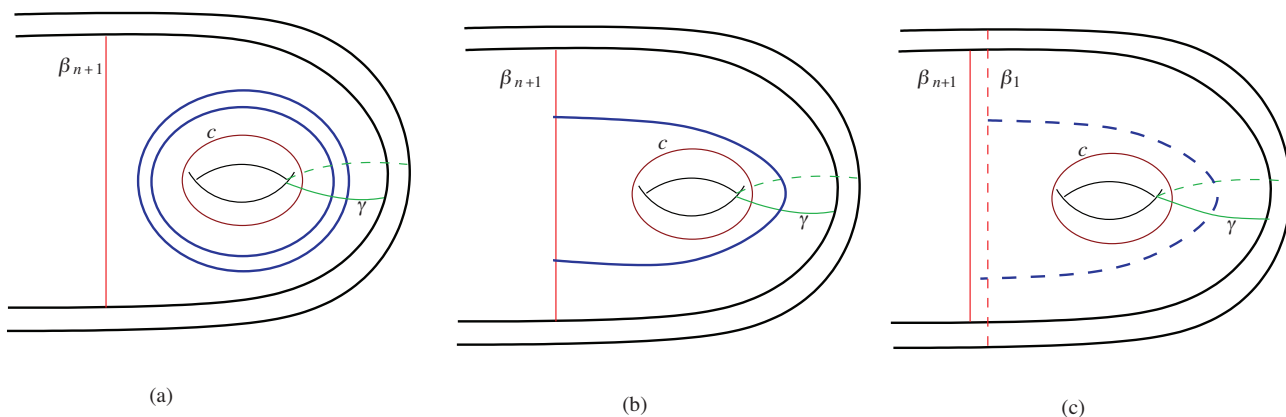


**Figure 4.** (a)  $c$  curves, (b) front genus component, (c) back genus component in the region  $G$ .

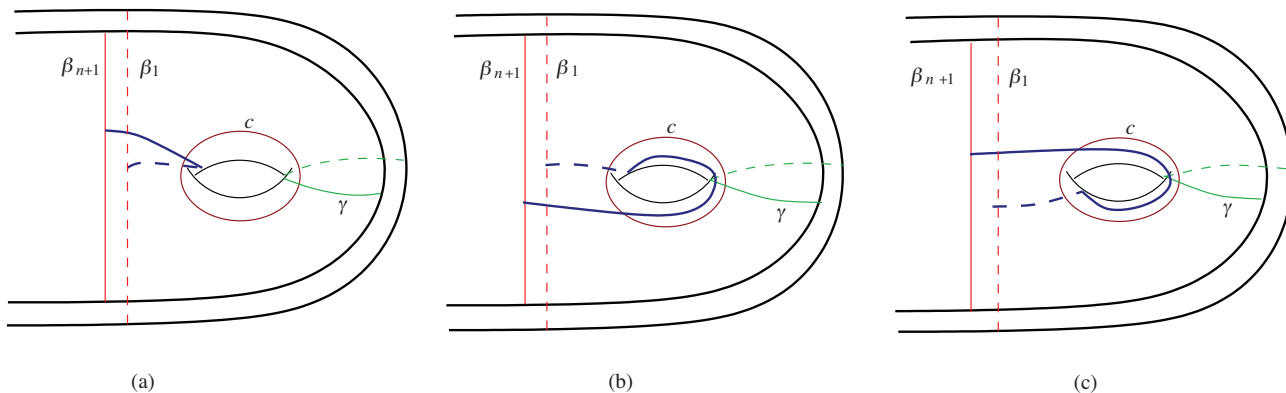


**Figure 5.** (a) Nontwist component, (b) negative twist component, (c) positive twist component.

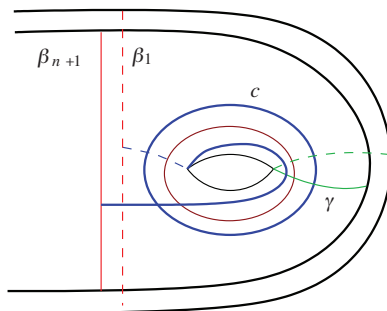


**Figure 6.** The integral lamination does not contain both the curve  $c$  and the twisting components at the same time.

$\max(c, 0)$  throughout the paper. That is, if the integral lamination contains the twisting components, then  $c > 0$  and the number of the twisting components is  $c^+$ ; if the integral lamination contains the curve  $c$ , then  $c < 0$  and the number of the copies of curve  $c$  is given by  $p(c)$ ; and if the integral lamination contains neither twisting components nor curve  $c$ , then  $c = 0$ .

**Remark 2.3** Since an integral lamination does not contain any self-intersections, the directions of the twists

have to be the same. Moreover, in the region  $G$ , the difference between the twist numbers of two different twisting components cannot be greater than 1 (see Figure 7).

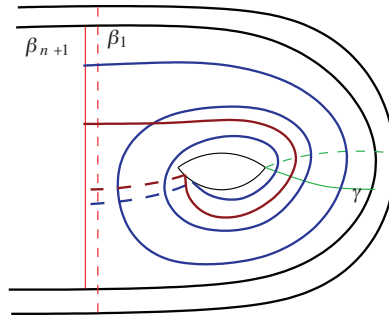


**Figure 7.** If the difference between the twist numbers of two twisting components is greater than one, then they intersect.

If we denote the smaller twist number by  $t$  and the bigger twist number by  $t + 1$ , then the total twist number  $T$  in  $G$  is the sum of the twist numbers of such components. Hence, if the difference between the twist numbers of any two twisting components is 0, then

$$T = tc^+.$$

On the other hand, if the difference between the twist numbers of any two twisting components is 1, then

$$T = m(t + 1) + (c^+ - m)t,$$

where  $m \in \mathbb{Z}_{\geq 0}$  is the number of the twisting components with the twist number  $t + 1$ , and  $c^+ - m$  is the number of the twisting components with the twist number  $t$ .

**Remark 2.4** Although  $T$  gives the total twist number in  $G$ , it cannot show the directions of the twists by itself. Therefore, we first calculate the number  $T$ , and then we add a sign in front of  $T$ , denoting the negative direction by  $-T$  and the positive direction by  $T$ . However, since only the total number of the twists is required in the formulas throughout the paper,  $|T|$  shall be used as the total number of the twists in order not to cause any confusion.

Now, we calculate the path components of  $L$  in  $G$ :

**Lemma 2.5** Let  $L$  be given with the intersection numbers  $(\alpha; \beta; \gamma; c)$ , and the number of the front genus components and the number of the back genus components be  $l$  and  $l'$ , respectively. Then,

$$l = \frac{\beta_{n+1} - c^+}{2} \quad \text{and} \quad l' = \frac{\beta_1 - c^+}{2}.$$

**Proof** The arc  $\beta_{n+1}$  intersects only with twisting (see Figure 5) and front genus (see Figure 4b) components. Since  $\beta_{n+1}$  intersects once with each twisting component and twice with each front genus component,  $\beta_{n+1} = c^+ + 2l$ . From here,  $l = \frac{\beta_{n+1} - c^+}{2}$  is derived. Similarly,  $\beta_1$  intersects only with twisting (see Figure 5) and back genus (see Figure 4c) components. Since  $\beta_1$  intersects once with each twisting component and twice with each back genus component,  $\beta_1 = c^+ + 2l'$ . Therefore,  $l' = \frac{\beta_1 - c^+}{2}$  is derived.  $\square$

In the following lemma, we calculate the total twist number of the twisting components:

**Lemma 2.6** *Let  $L$  be given with the intersection numbers  $(\alpha; \beta; \gamma; c)$ , denoting the signed total twist number of the twisting components by  $T$ . We have*

$$|T| = \begin{cases} 0 & \text{if } c^+ = 0, \\ \gamma - \frac{\beta_{n+1} - c^+}{2} - \frac{\beta_1 - c^+}{2} & \text{if } c^+ \neq 0. \end{cases} \quad (2.2)$$

*The sign of the negative twist component is  $-1$  and the sign of the positive twist component is  $1$ .*

**Proof** Let us denote the total twist number of twisting components of  $L$  by  $|T|$ . Note that the curve  $\gamma$  intersects once with curve  $c$  (see Figure 4a) and it intersects once with each front and back genus components (see Figures 4b and 4c, respectively). Moreover,  $\gamma$  intersects by the total number of twists of twisting components (see Figure 5) with  $L$ . However, from Remark 2.1, there cannot be twists and curve  $c$  at the same time. Therefore, when  $c^+ \neq 0$ , we have

$$\gamma = l + l' + |T|, \quad (2.3)$$

where  $l$ ,  $l'$ , and  $|T|$  denote the number of front genus, back genus components, and the total twist number of twisting components, respectively. From Lemma 2.5,

$$\gamma = \frac{\beta_{n+1} - c^+}{2} + \frac{\beta_1 - c^+}{2} + |T|.$$

Hence,

$$|T| = \gamma - \frac{\beta_{n+1} - c^+}{2} - \frac{\beta_1 - c^+}{2}.$$

□

By using the following lemma, we calculate the number of the curves  $c$  (see Figure 4a).

**Lemma 2.7** *Let  $L$  be given with the intersection numbers  $(\alpha; \beta; \gamma; c)$ . We find the number of the curves  $c$  in  $L$  with*

$$p(c) = \begin{cases} \gamma - \frac{\beta_{n+1}}{2} - \frac{\beta_1}{2} & \text{if } c^+ = 0, \\ 0 & \text{if } c^+ \neq 0. \end{cases} \quad (2.4)$$

**Proof** Whenever  $c^+ = 0$ , we can write  $\gamma = l + l' + p(c)$ . From Lemma 2.5,

$$l = \frac{\beta_{n+1}}{2} \quad \text{and} \quad l' = \frac{\beta_1}{2}.$$

Hence,  $p(c) = \gamma - \frac{\beta_{n+1}}{2} - \frac{\beta_1}{2}$  is derived. □

The twist numbers of each twisting component of an integral lamination whose intersection numbers are given are found by using Remark 2.3 and Lemma 2.6. We find these twist numbers with the following lemma.

**Lemma 2.8** *Let  $L$  be given with the intersection numbers  $(\alpha; \beta; \gamma; c)$ . Let  $|T|$  and  $m$  be the total twist number and the number of twisting components, each with  $t + 1$  twists, respectively. In this case,*

$$m \equiv |T| \pmod{c^+} \quad \text{and} \quad t = \frac{|T| - m}{c^+}, \quad (2.5)$$

where  $c^+ \neq 0$ .

**Proof** From Remark 2.3,

$$|T| = m(t + 1) + (c^+ - m)t.$$

From here, we have

$$|T| = m + tc^+.$$

Hence,

$$m \equiv |T| \pmod{c^+} \quad \text{and} \quad t = \frac{|T| - m}{c^+}$$

are derived.

□

**Remark 2.9** The intersection numbers  $(\alpha; \beta; \gamma; c)$  may not always give an integral lamination because intersection numbers may not provide the conditions given in Lemma 2.11 or Lemma 2.12, and the triangle inequality in each region bounded by  $\alpha_{2i-1}, \alpha_{2i}, \beta_i$  or by  $\alpha_{2i-1}, \alpha_{2i}, \beta_{i+1}$ .

As an example, we shall show that we cannot construct an integral lamination having the intersection numbers  $(1, 1, 1, 1, 1, 1; 0, 2, 0, 2; 2; 1)$  because, according to Lemma 2.5, the number of front genus and back genus components are respectively

$$l = \frac{\beta_4 - c^+}{2} = \frac{2 - 1}{2} = \frac{1}{2} \notin \mathbb{Z}_{\geq 0} \quad \text{and} \quad l' = \frac{\beta_1 - c^+}{2} = \frac{0 - 1}{2} = -\frac{1}{2} \notin \mathbb{Z}_{\geq 0}.$$

In such a case, an integral lamination cannot be constructed as shown in Figure 8.

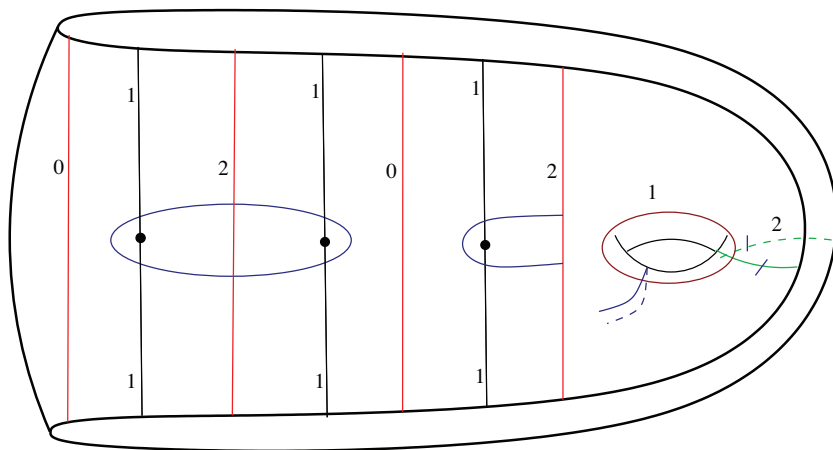


**Figure 8.** The arc  $\beta_i$  and  $\alpha_{2i} \cup \alpha_{2i-1}$  are each even; however,  $c$  is odd.

**Remark 2.10** In each region  $U_i$ , for  $1 \leq i \leq n$  let the number of the loop components be denoted by  $|b_i|$ , where

$$b_i = \frac{\beta_i - \beta_{i+1}}{2}. \tag{2.6}$$

If  $b_i < 0$ , the loop component is called left; if  $b_i > 0$ , the loop component is called right [4].

**Lemma 2.11** ([9]) *The following equalities hold for each  $U_i$ :*

*When there is a left loop component,*

$$\alpha_{2i} + \alpha_{2i-1} = \beta_{i+1}$$

$$\alpha_{2i} + \alpha_{2i-1} - \beta_i = 2|b_i|;$$

*when there is a right loop component,*

$$\alpha_{2i} + \alpha_{2i-1} = \beta_i$$

$$\alpha_{2i} + \alpha_{2i-1} - \beta_{i+1} = 2|b_i|;$$

*when there are no loop components,*

$$\alpha_{2i} + \alpha_{2i-1} = \beta_i = \beta_{i+1}.$$

**Lemma 2.12** *Let  $L$  be given with the intersection numbers  $(\alpha; \beta; \gamma; c)$ . Then for each  $1 \leq i \leq n$ ,  $\beta_i - \beta_{i+1}$  and  $\alpha_{2i} - \alpha_{2i-1} - c^+$  are even.*

**Proof** From Lemma 2.5, since

$$\beta_{n+1} = c^+ + 2l,$$

if  $c^+$  is even (odd),  $\beta_{n+1}$  is even (odd). Similarly, since

$$\beta_1 = c^+ + 2l',$$

if  $c^+$  is even (odd),  $\beta_1$  is even (odd). Moreover, from [4], the number of the loop components is given by

$$b_i = \frac{\beta_i - \beta_{i+1}}{2} \quad (1 \leq i \leq n).$$

Thus, we obtain

$$\beta_{i+1} = \beta_i - 2 \sum_{j=1}^i b_j.$$

Therefore, if  $c^+$  is even (odd), each  $\beta_i$  ( $1 \leq i \leq n + 1$ ) is even (odd). From Lemma 2.11, when there is the right loop component,  $\alpha_{2i} + \alpha_{2i-1} = \beta_i$ ; when there is the left loop component,  $\alpha_{2i} + \alpha_{2i-1} = \beta_{i+1}$ . Hence, when  $c^+$  is even (odd),  $\alpha_{2i} + \alpha_{2i-1}$  is even (odd). Therefore,  $\alpha_{2i} + \alpha_{2i-1} - c^+$  is always even. □

**Lemma 2.13** ([4]) *Let  $L \in \mathcal{L}_n$  be given with the intersection numbers  $(\alpha; \beta; \gamma; c)$ . For each  $1 \leq i \leq n$ , the number of above,  $u_i^a$ , and below,  $u_i^b$ , components in  $U_i$  can be found by*

$$u_i^a = \alpha_{2i-1} - |b_i| \quad \text{and} \quad u_i^b = \alpha_{2i} - |b_i|.$$

**Remark 2.14** *The intersection numbers of two different integral laminations might be equal.*



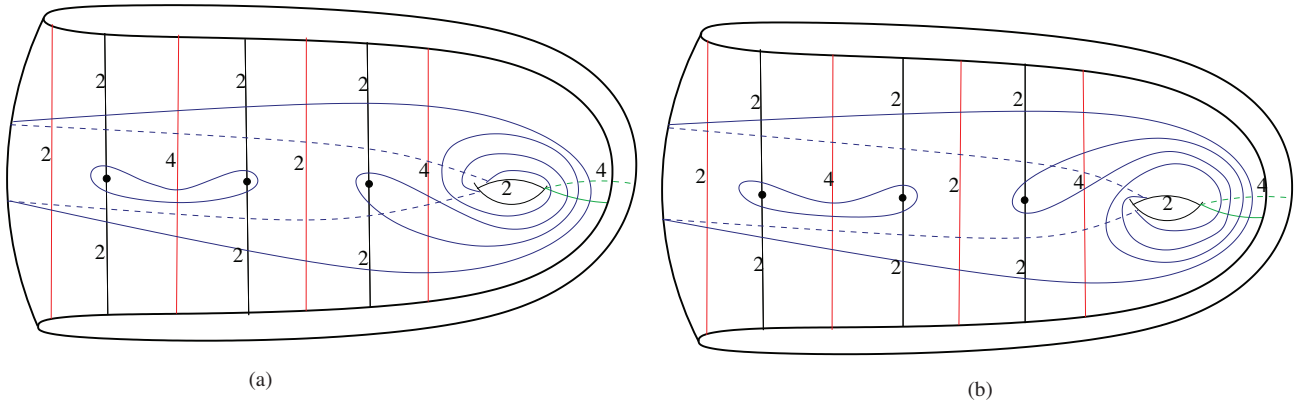


**Figure 9.** Two different integral laminations with the same intersection numbers.

For example, while the intersection numbers of two integral laminations given in Figure 9 are  $(2, 2, 2, 2, 2, 2; 2, 4, 2, 4; 4; 2)$ , since the twisting components of the integral lamination in Figure 9a twist in the negative direction and the twisting components of the integral lamination in Figure 9b twist in the positive direction, these integral laminations are different. We can derive an injective function from the intersection numbers  $(\alpha; \beta; \gamma; c)$  by giving a direction to the twisting components.

Let  $m_i = \min(\alpha_{2i} - |b_i|, \alpha_{2i-1} - |b_i|)$  and set  $2a_i = \alpha_{2i} - \alpha_{2i-1} - c^+$  for  $1 \leq i \leq n$ . By Lemma 2.12,  $a_i$  is an integer. By similar calculations as in the case of the disk, we can derive the intersection number with  $\alpha_i$  on  $S_n$  in the following way:

For each  $1 \leq i \leq 2n$ ,

$$\alpha_i = \begin{cases} \frac{2(-1)^i a_{\lceil i/2 \rceil} + (-1)^i c^+ + \beta_{\lceil i/2 \rceil}}{2} & \text{if } b_{\lceil i/2 \rceil} \geq 0, \\ \frac{2(-1)^i a_{\lceil i/2 \rceil} + (-1)^i c^+ + \beta_{(1+\lceil i/2 \rceil)}}{2} & \text{if } b_{\lceil i/2 \rceil} \leq 0, \end{cases} \tag{2.7}$$

where  $\lceil x \rceil$  is the smallest integer greater than or equal to  $x$ .

Now, we derive the intersection number with  $\beta_i$  on  $S_n$ . Let  $l, l'$ , and  $m_i$  ( $1 \leq i \leq n$ ) show the front genus, back genus, and the minimum of above and below component numbers, respectively. Since  $L$  cannot contain a parallel to the boundary, at least one of  $m_i, l$  or  $l'$  has to be 0. There are two cases:

**Case 1:** Assume at least one of  $m_i = 0$  for  $1 \leq i \leq n$ . In this case

$$\beta_{n+1} = \max_{1 \leq k \leq n} \left[ 2 \max(b_k, 0) + |2a_k + c^+| - 2 \sum_{j=k}^n b_j \right] \tag{2.8}$$

and

$$\beta_{n+1} \geq \max(c^+, c^+ - 2 \sum_{i=1}^n b_i). \tag{2.9}$$

An example for this case is depicted in Figure 10.

**Case 2:** If  $m_i \neq 0$  for any  $1 \leq i \leq n$ : In this case, an integral lamination contains curves whose above and below component numbers are different from 0 (see Figures 11a and 11b). Moreover, at least one of the

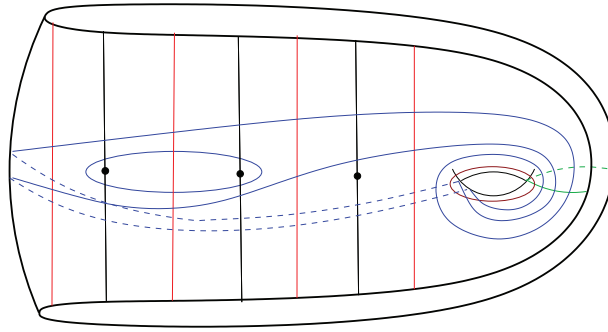


**Figure 10.** An integral lamination with  $m_i \neq 0$  for  $i = 1, 2$ .

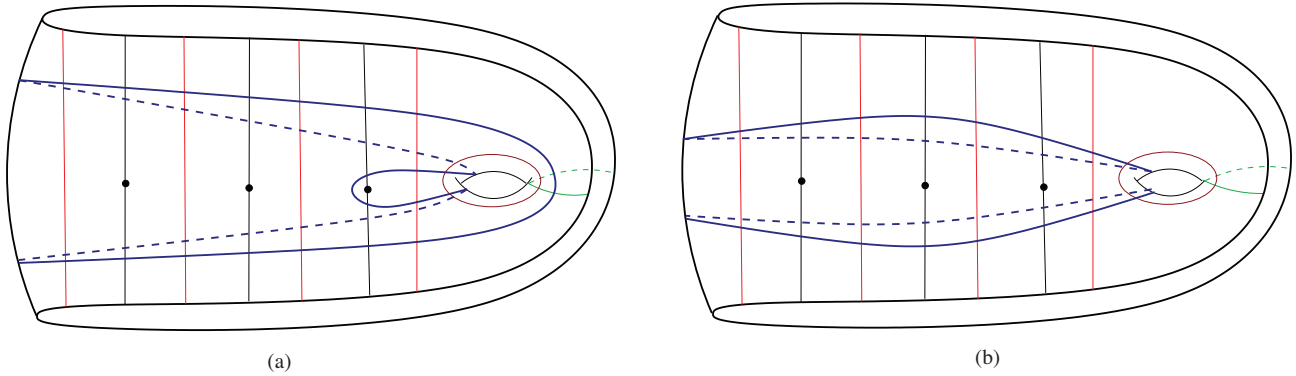


**Figure 11.** Integral laminations with each  $m_i$  different from 0.

front genus or the back genus component numbers must be 0. Otherwise, this curve system contains curves parallel to the boundary as shown in Figure 12.

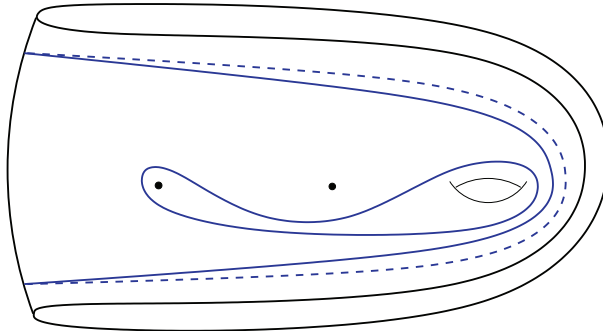


**Figure 12.** A curve system with a curve parallel to the boundary.

Therefore, there are three possibilities:

- (i) If  $l = l' = 0$  and  $\sum_{i=1}^n b_i = 0$ ,
- (ii) If  $l > 0$ ,  $l' = 0$  and  $\sum_{i=1}^n b_i < 0$ ,
- (iii) If  $l = 0$ ,  $l' > 0$  and  $\sum_{i=1}^n b_i > 0$ .

Combining cases (i), (ii), and (iii), we get

$$\beta_{n+1} = \begin{cases} c^+ - 2 \sum_{i=1}^n b_i & \text{if } \sum_{i=1}^n b_i < 0, \\ c^+ & \text{if } \sum_{i=1}^n b_i > 0, \\ c^+ & \text{if } \sum_{i=1}^n b_i = 0. \end{cases} \tag{2.10}$$

Since each  $m_i > 0$  for  $1 \leq i \leq n$ , we have

$$\beta_{n+1} \geq \max_{1 \leq k \leq n} \left[ 2 \max(b_k, 0) + |2a_k + c^+| - 2 \sum_{j=k}^n b_j \right]. \tag{2.11}$$

In terms of brevity, let

$$\kappa := \max_{1 \leq k \leq n} \left[ 2 \max(b_k, 0) + |2a_k + c^+| - 2 \sum_{j=k}^n b_j \right].$$

From inequalities (2.9) and (2.11), we have

$$\beta_{n+1} = \max(c^+, c^+ - 2 \sum_{i=1}^n b_i, \kappa). \tag{2.12}$$

From Equation (2.6), for each  $1 \leq i \leq n$ ,

$$\beta_i = 2 \sum_{j=i}^n b_j + \beta_{n+1}. \tag{2.13}$$

Now, we derive the intersection number with  $\gamma$  on  $S_n$ . Since each path component in the region  $G$ , except nontwist components (see Figure 5a), intersects the arc  $\gamma$  once, we have

$$\gamma = l + l' + p(c)$$

if  $p(c) \neq 0$ . From Remark 2.1, when  $p(c) = 0$ , we have

$$\gamma = l + l' + |T|.$$

Recall that from Equation (2.1),  $p(c) = -c$ . Therefore,

$$\gamma = \begin{cases} |T| + l + l' & \text{if } c > 0, \\ |c| + l + l' & \text{if } c \leq 0. \end{cases} \tag{2.14}$$

By Lemma 2.5, Equations (2.12) and (2.13), we have

$$\gamma = \begin{cases} |T| + \sum_{j=1}^n b_j + \max(c^+, c^+ - 2 \sum_{i=1}^n b_i, \kappa) - c^+ & \text{if } c > 0, \\ |c| + \sum_{j=1}^n b_j + \max(c^+, c^+ - 2 \sum_{i=1}^n b_i, \kappa) - c^+ & \text{if } c \leq 0. \end{cases} \tag{2.15}$$

Above we have expressed the intersection numbers with the arcs  $\alpha_i$ ,  $\beta_i$ , and  $\gamma$  in terms of  $a_i$ ,  $b_i$ , and  $T$ . Note that  $T = 0$  when  $c \leq 0$  for an integral lamination.

Now, we can define the Dynnikov coordinate system on  $S_n$ , which bijectively coordinates the set  $\mathcal{L}_n$ .

**Definition 2.15** Let  $\mathcal{V}_n = \{(a; b; T; c) : c \leq 0 \text{ and } T \neq 0\} \cup \{0\}$ . The Dynnikov coordinate function  $\Phi : \mathcal{L}_n \rightarrow \mathbb{Z}^{2n+2} \setminus \mathcal{V}_n$  on  $S_n$  is defined by

$$\Phi(L) = (a; b; T; c) = (a_1, \dots, a_n; b_1, \dots, b_n; T; c),$$

where for each  $1 \leq i \leq n$ ,

$$a_i = \frac{\alpha_{2i} - \alpha_{2i-1} - c^+}{2}, \quad b_i = \frac{\beta_i - \beta_{i+1}}{2} \tag{2.16}$$

and

$$|T| = \begin{cases} 0 & \text{if } c^+ = 0, \\ \gamma - \frac{\beta_{n+1} - c^+}{2} - \frac{\beta_1 - c^+}{2} & \text{if } c^+ \neq 0. \end{cases} \tag{2.17}$$

**Example 2.16** We calculate the Dynnikov coordinates of the integral lamination shown in Figure 2.

Since  $(\alpha_1, \alpha_2, \alpha_3, \alpha_4, \alpha_5, \alpha_6; \beta_1, \beta_2, \beta_3, \beta_4; \gamma; c) = (4, 1, 3, 2, 4, 1; 3, 5, 5, 3; 3; 1)$ , from Equations (2.16)

$$a_1 = \frac{\alpha_2 - \alpha_1 - c^+}{2} = \frac{1 - 4 - 1}{2} = -2,$$

$$a_2 = \frac{\alpha_4 - \alpha_3 - c^+}{2} = \frac{2 - 3 - 1}{2} = -1,$$

$$a_3 = \frac{\alpha_6 - \alpha_5 - c^+}{2} = \frac{1 - 4 - 1}{2} = -2,$$

$$b_1 = \frac{\beta_1 - \beta_2}{2} = \frac{3 - 5}{2} = -1,$$

$$b_2 = \frac{\beta_2 - \beta_3}{2} = \frac{5 - 5}{2} = 0,$$

$$b_3 = \frac{\beta_3 - \beta_4}{2} = \frac{5 - 3}{2} = 1.$$

Moreover, since  $c^+ = \max(c, 0) = \max(1, 0) = 1$ , from Equation (2.17),

$$|T| = \gamma - \frac{\beta_4 - c^+}{2} - \frac{\beta_1 - c^+}{2} = 3 - \frac{3 - 1}{2} - \frac{3 - 1}{2} = 1.$$

Since the twisting component twists in the negative direction, we derive  $T = -1$ . Hence, we find

$$\Phi(L) = (-2, -1, -2; -1, 0, 1; -1; 1).$$

The following theorem gives the inversion of the Dynnikov coordinate function on  $S_n$ .

**Theorem 2.17** Let  $(a; b; T; c) \in \mathbb{Z}^{2n+2} \setminus \mathcal{V}_n$ . Then, the vector  $(a; b; T; c)$  corresponds to one and only one integral lamination  $L \in \mathcal{L}_n$  whose intersection numbers are given by

$$\beta_i = 2 \sum_{j=i}^n b_j + \max(c^+, c^+ - 2 \sum_{i=1}^n b_i, \kappa), \quad \beta_{n+1} = \max(c^+, c^+ - 2 \sum_{i=1}^n b_i, \kappa), \tag{2.18}$$

$$\alpha_i = \begin{cases} \frac{2(-1)^i a_{\lceil i/2 \rceil} + (-1)^i c^+ + \beta_{\lceil i/2 \rceil}}{2} & \text{if } b_{\lceil i/2 \rceil} \geq 0, \\ \frac{2(-1)^i a_{\lceil i/2 \rceil} + (-1)^i c^+ + \beta_{(1+\lceil i/2 \rceil)}}{2} & \text{if } b_{\lceil i/2 \rceil} \leq 0, \end{cases} \tag{2.19}$$

and

$$\gamma = \begin{cases} |T| + \sum_{j=1}^n b_j + \max(c^+, c^+ - 2 \sum_{i=1}^n b_i, \kappa) - c^+ & \text{if } c > 0, \\ |c| + \sum_{j=1}^n b_j + \max(c^+, c^+ - 2 \sum_{i=1}^n b_i, \kappa) - c^+ & \text{if } c \leq 0, \end{cases} \tag{2.20}$$

where

$$\kappa = \max_{1 \leq k \leq n} \left[ 2 \max(b_k, 0) + |2a_k + c^+| - 2 \sum_{j=k}^n b_j \right].$$

**Proof** Let  $L \in \mathcal{L}_n$  be an integral lamination whose Dynnikov coordinates are  $\Phi(L) = (a; b; T; c)$ . First, we shall show that the Dynnikov coordinate function  $\Phi : \mathcal{L}_n \rightarrow \mathbb{Z}^{2n+2} \setminus \mathcal{V}_n$  is injective. We have already shown in this paper that the intersection numbers corresponding to the minimal representative  $L \in \mathcal{L}$  are as given in Equations (2.18), (2.19), and (2.20). Then, the numbers of above, below, right loop or left loop components in each region  $U_i$ , the numbers of curves  $c$ , front genus, back genus, twisting components, the total twist of twisting components and the number of twists of each twisting component, the direction of these twists in the region  $G$  are calculated as given in above and the path components in the regions  $U_i$  and  $G$  are combined uniquely up to isotopy by giving a direction to the twisting components. Hence,  $\Phi$  is injective.

Now, we see that the function  $\Phi : \mathcal{L}_n \rightarrow \mathbb{Z}^{2n+2} \setminus \mathcal{V}_n$  is surjective. Let  $(a; b; T; c) \in \mathbb{Z}^{2n+2} \setminus \mathcal{V}_n$ . We shall show that the intersection numbers  $(\alpha; \beta; \gamma; c)$  defined by Equations (2.18), (2.19), and (2.20) correspond to an integral lamination  $L \in \mathcal{L}_n$  such that  $\Phi(L) = (a; b; T; c)$ . First, it is easy to see that an integral lamination  $L$  with the intersection numbers  $(\alpha; \beta; \gamma; c)$  should satisfy  $\Phi(L) = (a; b; T; c)$ . In order to get an integral lamination, we draw nonintersecting path components in each region and join them together.  $\square$

**Example 2.18** Let the Dynnikov coordinates of the integral lamination  $L \in \mathcal{L}_3$  on  $S_3$  be

$$\Phi(L) = (a; b; T; c) = (-2, -2, -1; 0, -1, -1; -5; 3).$$

We find the intersection numbers corresponding to the minimal representative  $L$ .

Since  $c = 3 > 0$ ,  $p(c) = 0$ , and  $c^+ = 3$ . From Theorem 2.17, the intersection numbers  $\alpha$ ,  $\beta$ , and  $\gamma$  are found as follows:

When we substitute the given Dynnikov coordinates to the equation

$$\kappa = \max_{1 \leq k \leq 3} \left[ 2 \max(b_k, 0) + |2a_k + c^+| - 2 \sum_{j=k}^3 b_j \right],$$

we find  $\kappa = 5$ . From here,

$$\begin{aligned} \beta_4 &= \max(c^+, c^+ - 2 \sum_{i=1}^3 b_i, \kappa) \\ &= \max(3, 3 - 2(0 - 1 - 1), 5) = 7; \end{aligned}$$

hence,  $\beta_4 = 7$ . From Equation (2.13), we derive

$$\beta_1 = 2(b_1 + b_2 + b_3) + \beta_4 = 2(0 - 1 - 1) + 7 = 3.$$

In a similar vein, we have  $\beta_2 = 3$  and  $\beta_3 = 5$ . From Equation (2.19), we find  $\alpha_1 = 2$ ,  $\alpha_2 = 1$ ,  $\alpha_3 = 3$ ,  $\alpha_4 = 2$ ,  $\alpha_5 = 3$  and  $\alpha_6 = 4$ . Since  $c > 0$ , from Equation (2.20),

$$\begin{aligned} \gamma &= |T| + \sum_{j=1}^3 b_j + \max(c^+, c^+ - 2 \sum_{i=1}^3 b_i, \kappa) - c^+ \\ &= |T| + b_1 + b_2 + b_3 + \max(c^+, c^+ - 2(b_1 + b_2 + b_3), \kappa) - c^+ \\ &= 5 + 0 - 1 - 1 + \max(3, 3 - 2(0 - 1 - 1), 5) - 3 = 7. \end{aligned}$$

Now, we calculate the number of the path components in the regions  $G$  and  $U_i$ . Since  $c^+ = 3$  and  $T = -5$ , there are 3 twisting components and the total number of twists is 5 (see Remark 2.2 and Lemma 2.6), and observe that the twisting components twist in the negative direction. By Lemma 2.8, there are 2 twisting components, which each twisting component does 2 twists, and there is 1 twisting component doing 1 twist as depicted in Figure 13. Each of the purple and pink twisting components does 2 twists and the green twisting component does 1 twist. According to Lemma 2.5,

$$l = \frac{\beta_4 - c^+}{2} = \frac{7 - 3}{2} = 2 \quad \text{and} \quad l' = \frac{\beta_1 - c^+}{2} = \frac{3 - 3}{2} = 0.$$

That is, there are 2 front genus components; however, there is not any back genus component (Figure 13). From Equation (2.6),

$$b_1 = \frac{\beta_1 - \beta_2}{2} = \frac{3 - 3}{2} = 0.$$

Similarly, we have  $b_2 = -1$  and  $b_3 = -1$ . Namely, there are no loop components in the region  $U_1$ , 1 left loop component in the region  $U_2$ , and 1 left loop component in the region  $U_3$  (Figure 13). The numbers of above and below components in each  $U_i$  are:

$$u_1^a = \alpha_1 - |b_1| = 2 - 0 = 2 \quad \text{and} \quad u_1^b = \alpha_2 - |b_1| = 1 - 0 = 1.$$

Thus, there are 2 above components and 1 below component in  $U_1$ . Similarly, we find 2 above components and 1 below component in  $U_2$ , and 2 above and 3 below components in  $U_3$  (Figure 13). The integral lamination  $L$  in Figure 14 is derived uniquely by combining the calculated path components (Figure 13) up to isotopy. The integral lamination in this example (Figure 14) is a disconnected integral lamination consisting of two connected components (green and purple essential simple closed curves).

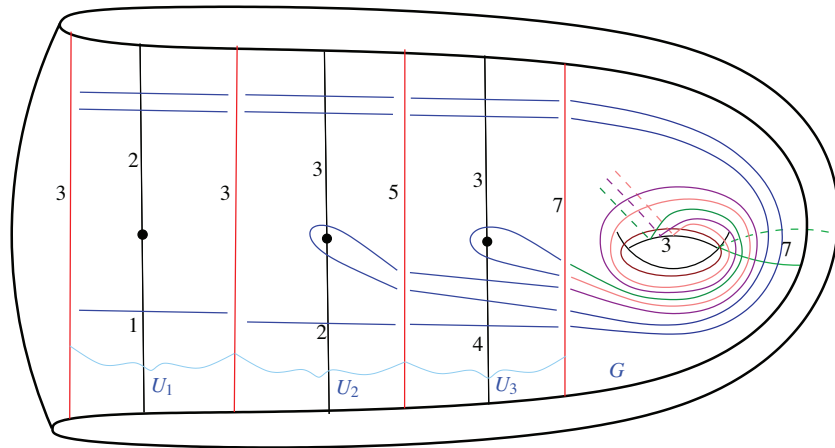


Figure 13. Path components in each  $U_i$  and  $G$

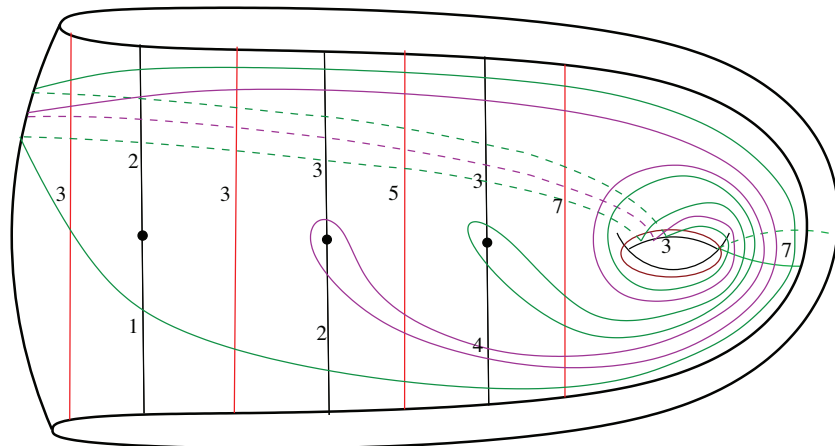


Figure 14.  $\Phi(L) = (a; b; T; c) = (-2, -2, -1; 0, -1, -1; -5; 3)$ .

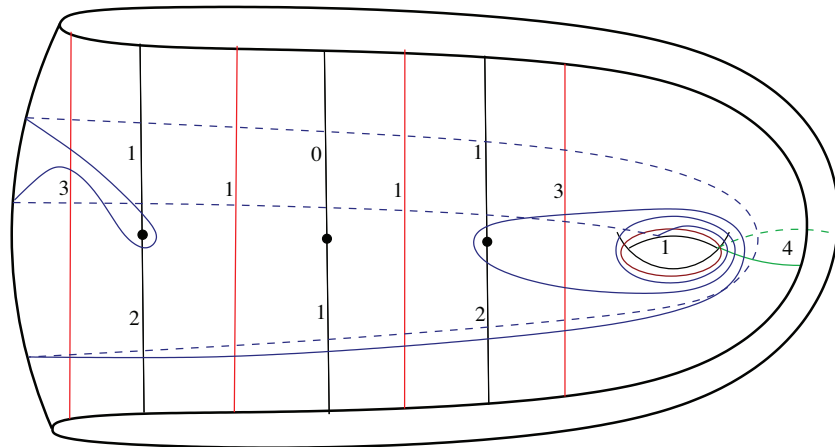


Figure 15.  $\Phi(L) = (a; b; T; c) = (0, 0, 0; 1, 0, -1; -2; 1)$ .

An integral lamination is connected if it consists of only one closed curve. For example, the integral lamination  $L$  on  $S_3$  in Figure 15 is a connected integral lamination which has Dynnikov coordinates  $(0, 0, 0; 1, 0, -1; -2; 1)$  defined in Definition 2.15.

We can draw the integral lamination corresponding to the coordinates  $a_i$ ,  $b_i$ ,  $T$ , and  $c$  in a unique way. That is, geometrically,  $a_i$  helps us find the difference between the below and above component numbers in the region  $U_i$ .  $b_i$  gives the loop component numbers in that region and the sign of  $b_i$  indicates that these loop components are left or right.  $T$  is the total number of twists in the region  $G$  of this integral lamination, and the sign of  $T$  tells the direction of these twists which is negative or positive. If  $c > 0$ , there are twisting components in this lamination, and the number of  $c$  is the number of these components. If  $c < 0$ , there are curves  $c$  and the absolute value of  $c$  gives the number of these curves. If  $c = 0$ , there are not both twisting components and curve  $c$  in this lamination. For example, since  $a_1 = -2$  in Example 2.18, we see that  $u_1^b + 1 = u_1^a$ . Thus, in the region  $U_1$ , the number of above components is 1 more than the number of below components. Since  $b_2 = -1$ , there is 1 left loop component in  $U_2$ . Since  $c = 3$ , there are 3 twisting components in this lamination. Moreover, since  $T = -5$  in  $G$ , the total twist number of these twisting components is 5 and the direction of these twists is negative. In line with this information, when we place the path components on the surface  $S_3$  and join them together, one and only one integral lamination is derived as we proved in Theorem 2.17. After the integral lamination is obtained in this way, it is understood that this lamination is disconnected or connected.

**Remark 2.19** *The Dynnikov coordinates for the integral laminations on  $S_n$  obtained can be extended in a natural way to the Dynnikov coordinates of the measured foliations on  $S_n$ .*

## Acknowledgments

The author would like to thank her advisor Saadet Öykü Yurttaş and coadvisor Semra Pamuk and point out that the results in this paper are part of the author's PhD thesis. The author is also grateful to the anonymous referee and to the editor for helpful comments and suggestions on earlier versions of this paper. The author would also like to express her sincere thanks to her postdoctoral advisor Mustafa Korkmaz for his valuable suggestions and comments.

## References

- [1] Bestvina M, Handel M. Train-tracks for surface homeomorphisms. *Topology* 1995; 34 (1): 109-140.
- [2] Dehornoy P. Efficient solutions to the braid isotopy problem. *Discrete Applied Mathematics* 2008; 156 (16): 3091-3112.
- [3] Dehornoy P, Dynnikov I, Rolfsen D, Wiest B. *Ordering Braids*. Providence, RI, USA: American Mathematical Society, 2008.
- [4] Dynnikov I. On a Yang-Baxter map and the Dehornoy ordering. *Russian Mathematical Surveys* 2002; 57 (3): 592-594.
- [5] Haas A, Susskind P. The connectivity of multicurves determined by integral weight train tracks. *Transactions of the American Mathematical Society* 1992; 329 (2): 637-652.
- [6] Hamidi-Tehrani H, Chen Z. Surface diffeomorphisms via train-tracks. *Topology and its Applications* 1996; 73 (2): 141-167.
- [7] Moussafir J. On computing the entropy of braids. *Functional Analysis and Other Mathematics* 2006; 1 (1): 37-46.
- [8] Penner RC, Harer JL. *Combinatorics of Train Tracks*. Annals of Mathematics Studies. Princeton, NJ: Princeton University Press, 1992.



- [9] Yurttas SÖ, Hall T. On the topological entropy of families of braids. *Topology and its Applications* 2009; 158 (8): 1554-1564.
- [10] Yurttas SÖ. Geometric intersection of curves on punctured disks. *Journal of the Mathematical Society of Japan* 2013; 65 (4): 1554-1564.
- [11] Yurttas SÖ, Hall T. Intersections of multicurves from Dynnikov coordinates. *Bulletin of Australian Mathematical Society* 2018; 98 (1): 149-158.